Full Paper

Control of Stepwise Hg^{2+} Reduction on Gold to Selectively Tune Its Peroxidase and Catalase-like Activities and the Mechanism

Yao Chen,[a,‡] Xiaomei Shen,[b,‡] Unai Carmona,[c] Fan Yang,[c] Xingfa Gao,[,b] Mato Knez*[,c] and Lianbing Zhang*[,a], Yong Qin[a]*

Dr. Y. Chen, and Prof. L. Zhang
School of Life Sciences,
Northwestern Polytechnical University,
Xi'an, 710072, China
E-mail: lbzhang@nwpu.edu.cn

Dr. X. Shen and Prof. X. Gao
College of Chemistry and Chemical Engineering,
Jiangxi Normal University,
Nanchang, 330022, China
E-mail: gaox@jxnu.edu.cn

Dr. U. Carmona, Dr. F. Yang and Prof. M. Knez
CIC nanoGUNE Consolider,
Tolosa Hiribidea 76,
20018 Donostia-San Sebastian, Spain

IKERBASQUE,
Basque Foundation for Science,
Alameda Urquijo 36-5, 48011 Bilbao, Spain
Email: m.knez@nanogune.eu

Keywords: Au nanozyme, mercury treatment, Au@Hg amalgam, nanozymatic activity, activity specificity adjustment

Abstract: The flexible regulation of enzyme-like activities of nanozyme is of great importance in biomedical applications. However, the current modulation strategies usually lack activity specificity to reveal precise tuning of the desired activity. In this work, we demonstrated for the first time that the Hg^{2+} on surfaces of Au film could be reduced in a

chemical path of Hg(II) → Hg(I) → Hg(0) via anti-Galvanic reaction. Furthermore, it is amazing that the generated Hg^0 via $Hg(NO_3)_2$ treatment contributes to greatly boosted peroxidase and catalase activities of Au films due to formation of Au@Hg amalgam, while the main Hg^+ species on Au formed by $HgCl_2$ modification results in only catalase-like activity acceleration. Basing on this, the peroxidase- and catalase-like activities of gold can be selectively modulated by controlling the stepwise reduction of Hg^{2+}. Further density functionality theory (DFT) calculations reveal that it is the significantly lowered activation energy by Au@Hg amalgam that accounts for the acceleration of both peroxidase and catalase reaction. These results demonstrated a novel avenue to specifically modulate the enzyme-mimicking activities of Au, which not only facilitate the design of nanozymes with specific activity, but also broaden their biological usage.

1. Introduction

The great advance of nanotechnology and biotechnology provides new avenues for the design and synthesis of nanomaterials with biological enzyme-like catalytic activity. Since the pioneering work by Yan[1] that chemically inert Fe_3O_4 nanoparticles possess unexpected peroxidase-like activity, countless nanomaterial-based artificial enzymes (named nanozyme) were developed to imitate the catalytic functions of oxidases[2], peroxidases[3], superoxide dismutase[4] and catalase[5]. Owing to their merits of simple synthesis procedure with low cost, good stability, multiple functions, as well as good robustness under extreme conditions, nanozymes have been considered as next-generation synthetic enzymes and attracted great attention worldwide[6].

Unlike natural enzymes, the enzyme-mimicking activities of nanozymes can be modulated by the size, morphology, composition, as well as surface engineering with

numerous strategies [7]. In consequence, stimulatory or inhibitory effects on enzyme mimetic activities can be realized due to changes in surface physical and electronic properties, active sites accessibility, substrates affinity and production desorption. Nevertheless, the currently reported methods still lack activity specificity, which always simultaneously accelerate or decrease multiple activities. This, to some extent, hampers its further application closely related to specific and desired nanozymatic activity.

Recently, gold nanozyme has gained special interest due to its unique physiochemical and optical characteristics and exhibit high utilization value in biomedical applications. As both peroxidase and catalase mimetics, its relatively low activities were upregulated by a serial of modulators, such as bovine serum albumin, ATP, hemin, ions, metals and carbon nanomaterials[3b, 8]. In particular, some heavy metal ions like Ag^{+}, Bi^{3+} and Hg^{2+} were demonstrated to be the promising activators to reveal remarkable enhancement in enzyme-like activities.[9] For instance, the catalase-like activity of AuNPs was strongly increased by over 100 hundred fold after surface deposition of Hg^{2+}.[10] However, the possible interactions between metal ions and gold, as well as the exact activation mechanism remain unclear and need to be fully elucidated. More seriously, the heavy metal ions accelerate simultaneously both peroxidase and catalase activity, which is harmful if only one specific activity is desired. Taking nanozymatic-catalytic therapy for example, the $^{\cdot}OH$ generation from peroxidase reaction is a great hindrance to the elimination of the relatively high levels of reactive oxygen species by the catalase-like function, vice versa. Hence, it is imperative to understand the activation mechanism and thereby develop an effective modulator to realize specific activity regulation of gold.

In this work, we report, for the first time, the selectively modulating of the peroxidase- and catalase-like activities of gold nanozyme by controlling the stepwise reduction of Hg^{2+}

originated from different precursors. A chemical inert gold thin film coated on silicon wafer with bulk scale was first adopted as stable and recyclable gold sample. We demonstrated a stepwise reduction of Hg^{2+} on surfaces of Au film in a chemical path of Hg(II) → Hg(I) → Hg(0) via anti-Galvanic reaction (AGR). It is amazing that $Hg(NO_3)_2$ treated Au films present greatly boosted peroxidase and catalase activities due to formation of Au@Hg amalgam, while $HgCl_2$ treated ones display only catalase-like activity acceleration for its major Hg^{+} species on Au surface. Hence a selective modulation avenue for peroxidase and catalase activities regulation can be achieved by adjusting the Hg^{2+}-containing precursors. Further density functionality theory (DFT) calculations were also conducted to reveal the underlying mechanism for this activating effect, which implies that the activation energy for both peroxidase and catalase reaction were significantly lowered by Au@Hg amalgam.

2. Experimental

Chemicals and Materials. $HgCl_2$, $Hg(NO_3)_2$ and all chemicals used were purchased from Sigma. 3,3',5,5'-Tetramethylbenzidine (TMB) and Hydrogen peroxide (H_2O_2) were obtained from J&K Scientific. Commercial silicon wafers with a thickness of 5 μm and diameter of 80 mm were purchased from Zhejiang Jingli. All materials were used as received without any further treatment.

Instrumentation. The surface morphologies of gold thin layer samples were examined by scanning electron microscopy (FEI, Quanta 250 FEG). The crystal structure was analyzed by X-ray diffraction (XRD) with a MAXima XRD-7000 diffractometer. The ultraviolet visible (UV-Vis) absorption spectra were recorded by using a NanoDrop OneC (Thermo).

Synthesis of gold thin layer. We used silicon wafers as substrates to prepare thin gold films. Prior to use, the wafers were cut into 10 mm square pieces and soaked in piranha solution for

3 h, followed by rinsing with deionised water multiple times. The Au films were fabricated by using a radio frequency magnetron spattering method at room temperature.

Hg^{2+} treatment. The Hg^{2+} treatment was carried out by incubating silicon wafers with thin gold layers in $HgCl_2$ or $HgNO_3$ solutions (2 mM) over night. In order to exclude the possible interference from the Hg^{2+} residues, the treated samples were washed several times with deionized water after $HgCl_2$ or $Hg(NO_3)_2$ treatment, following by immersing in deionized water for two days.

Gold thin layer treated with ammonia. The ammonia (28 wt%) was stored in a glass jar. It is easy to achieve ammonia vapor saturation due to its high volatility. The gold thin layers were exposed to the ammonia vapor for 2 s.

Peroxidase-activity Assay. The peroxidase activity was determined with a typical colorimetric method. Briefly, 2 ml NaOAc buffer (0.2 M, pH 3.6), containing 50 μM TMB and 1 mM H_2O_2 was mixed in a tube. Then a piece of Au-coated wafer was added to the solution and incubated at 37 ºC for 30 min. The reaction was terminated by removing the wafer from the solution and the UV-vis absorption spectra of the oxidized TMB at 650 nm were immediately recorded.

Catalase-activity Assay. For thin gold layers, a H_2O_2 solution (30 wt%) was directly dropped on the gold surfaces and the catalase activity was judged by observing the O_2 bubbling reaction. The results were recorded with a camera. The catalase activities of the samples were also examined by monitoring the absorbance change of H_2O_2 at 240 nm. Typically, a Au coated wafer was added to 1 mL phosphate saline buffer (0.01 M, pH 7.4) containing 1 mM H_2O_2, and the reaction kinetics was recorded at 37 ºC for 10 min in a scanning kinetic mode.

Theoretical calculations. To model the gold surface with mercury treatment, structures with Hg^{2+} deposited on face-centered cubic site of four-layered (4×4) unit cell Au(111) slab were

selected. The geometries were optimized by the Vienna ab initio Simulation Package (VASP)[11] with Perdew-Burke–Ernzerhof (PBE) of generalized gradient approximation (GGA) exchange-correlation functional[12] of Projector augmented wave (PAW) potential[13]. During the calculations, the bottom two layers of atoms were kept fixed and the others were relaxed. 400 eV energy cut-off and 0.2 eV first-order Methfessel-Paxton[14] smearing were used. And the vacuum height was set to 15 Å for all structures. Monkhorst-Pack mesh k-points[15] were sampled with (3×3×1) for all calculations. The conjugated-gradient algorithm was used to optimize structures until the energies and forces converged up to 10^{-6} and 0.02 eV/Å, respectively. Spin polarized calculations were performed for O_2-involving structures. For other structures, spin unpolarized calculations were performed. Adsorption energies were calculated with

$$E_{ads} = E_{Au@Hg+mol} - (E_{Au@Hg} + E_{mol})$$

where E_{mol} represents the energy of adsorbates, such as H_2O_2, OH·, $E_{Au@Hg}$ represents the energy of bare Au(111) surface with deposited Hg^{2+}, and the $E_{Au@Hg+mol}$ represents the total energy of Au(111)@Hg surface with adsorbate adsorption it.

3. Results and discussion

In order to elucidate the activating mechanism of heavy metal ions on enzyme-mimicking activities of gold, it is critical to investigate the surface properties change after treatment. In this study, a gold thin layer coated on the surface of a commercial silicon wafer was firstly adopted as gold sample to clear identify the surface property change after Hg^{2+} treatment, which can also overcome the shortcoming that it is difficult to achieve purified ultrafine Au nanoparticles after treatment. XRD examination reveals that, on surfaces of bare gold film, there is a main peak located at 2θ of 38° in the XRD spectra (Fig. S1),

corresponding to Au (111). For the Hg^{2+} treatment, the silicon wafer with the thin gold layer was firstly immersed in $HgCl_2$ solution overnight, followed by rinsing with water to remove residual Hg^{2+}. The images of the samples before and after treatment with Hg^{2+} are presented in Fig. 1A. The untreated sample (on the left-hand side) shows the typical gold-colored, mirror-like surface. The AFM picture (Fig. S2) show that a uniform distribution of Au particles with grain sizes around 10-20 nm in diameter and 4.9 nm in height are deposited on silica wafer. However, the gold layer became rough after the Hg^{2+} treatment and some white dots emerged on the gold surface (right hand side in Fig. 1A). In the SEM image some irregular crystal-like structures were observed (Fig. 1B), which were not present on the clean and flat surface of the untreated sample (Fig. S3). These crystals formed on the Au surfaces keep stable even after incubation in water for a week with only a small fraction of them being dissolved (Fig. S4). EDX spectra of those features reveal the addition of mercury element on Au film after $HgCl_2$ treatment (Fig S5). Further XPS characterization demonstrated that the Au4f XPS spectra for both treated and untreated Au films show two main peaks locating at 84.3 eV and 87.2 eV, which corresponds to $Au4f_{7/2}$ and $Au4f_{5/2}$, respectively and suggests their metallic Au^0 state (Fig 1F). Deconvolution of Hg4f core level spectra suggests the existence of two components of Hg^+ and Hg^0 on surfaces of $HgCl_2$-treated Au (Fig 1G), indicating Hg^+ as the possible intermediate by the reduction of Hg^{2+} to Hg^0.

Since the treatment solution contained only $HgCl_2$ salt, we suspected that these Hg-containing crystals were insoluble mercurous chloride (Hg_2Cl_2). In order to verify this conjecture, the treated sample was probed with a classical reaction:

$$Hg_2Cl_2 + NH_3 \rightarrow Hg(NH_2)Cl + Hg + NH_4Cl$$

Ammonia can disproportionate Hg_2Cl_2 to form Hg and Hg^{2+}. As shown in Fig. 1E, with short exposure to ammonia vapor, the Hg^{2+} treated sample (on the right-hand side) turned

black, while no changes were observed from the untreated sample (left-hand side). The color change was caused by the formation of small Hg particles. This observation confirmed that the Au films after $HgCl_2$ treatment is dominated by Hg_2Cl_2 crystals. We also performed density functional theory (DFT) calculations to study the energy changes for the chemisorption of $HgCl_2$ molecules on an Au(111) surface. The result suggested that the conversion of two $HgCl_2$ molecules to one Hg_2Cl_2* and two Cl* species on the Au surface is energetically favorable with a reaction energy of −1.18 eV (Fig. 1D). In contrast, the formation of one Hg_2* and four Cl^* is less favorable, with a reaction energy of −0.98 eV (Fig. 1E), matching well with the aforementioned experimental observations of the insoluble Hg_2Cl_2 crystals generated on the gold surface.

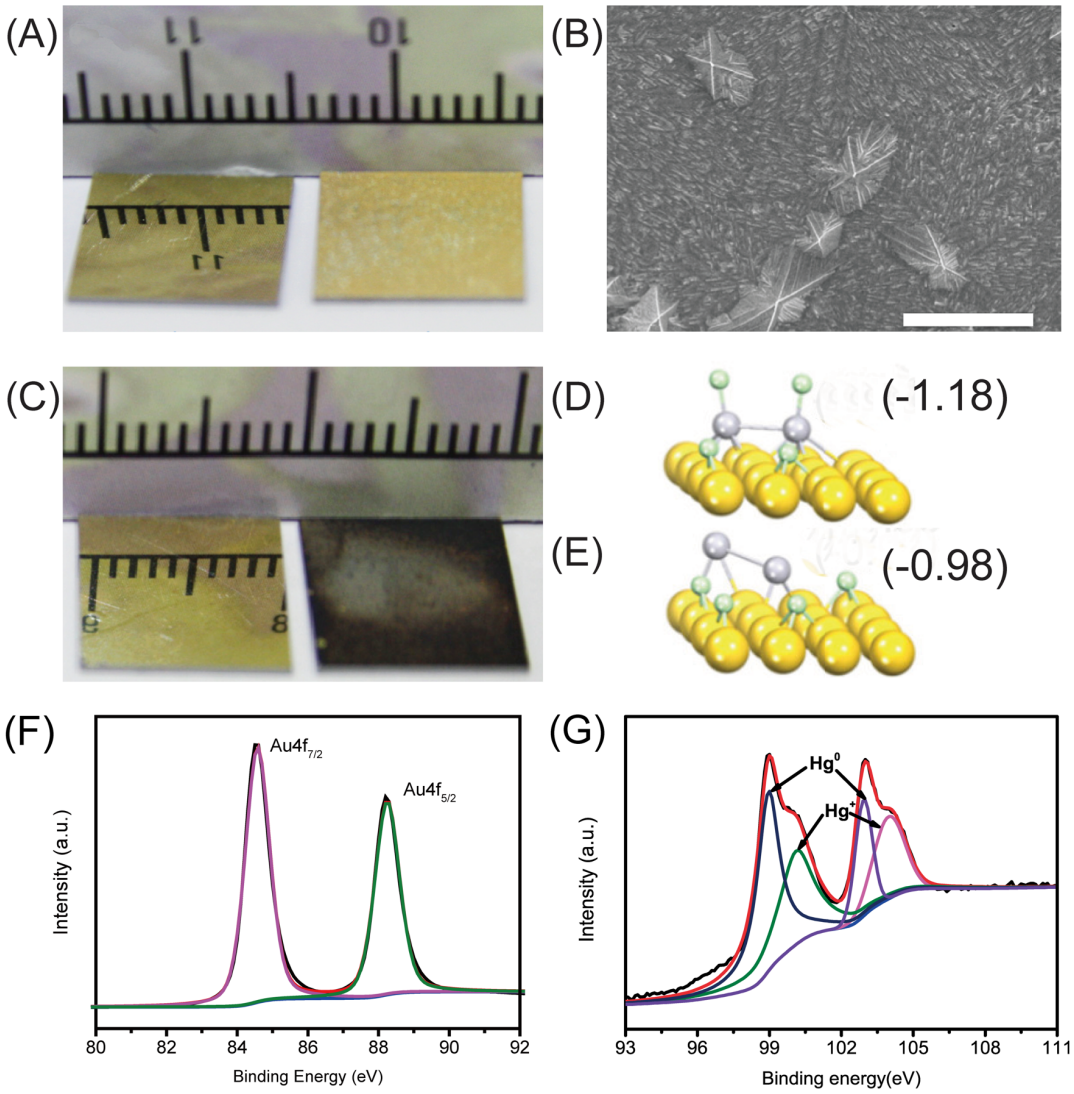

Figure 1. (A) Photograph of sputtered gold layers before (left) and after (right) treatment. (B) SEM image of a $HgCl_2$-treated sample, scale bar: 50 μm. (C) Image of gold surface after being exposed to ammonia vapor. The left one and the right one are gold layers without and with $HgCl_2$ treatment, respectively. (D) The computationally optimized structure for Hg_2Cl_2* and 2 Cl* species on the Au(111) surface. (E) The computationally optimized structure for Hg_2* and 4 Cl* species on the Au(111) surface. In (D) and (E), the adsorption energies are given in parentheses; the yellow, grey, and cyan atoms denote Au, Hg, and Cl, respectively.

The XPS core level of Au4f (F) and Hg4f (G). The Hg/Au ratio in $HgCl_2$ treated Au film determined by XPS is 8.77%.

In order to see whether Hg(I) can be further reduced to Hg(0) and to obviate the formation of insoluble Hg_2Cl_2, $Hg(NO_3)_2$ was then used as the Hg^{2+} source for the treatment. After the treatment no white dots were observed on the gold layer surfaces (Fig. 2A), since potentially formed $Hg_2(NO_3)_2$ is soluble. However, some islands in the size range of 10-50 nm were observed from the SEM images, as shown in Fig. 2B. EDX characterization of Fig. 2B strongly suggested the addition of Hg element on the treated gold surface. The elemental map of Au (Fig. 2C) and Hg (Fig. 2D) demonstrates that these islands are formed by homogenous Au@Hg alloys, but not Hg islands. Hence, they might result from the formation of an Au-Hg amalgam, which uniformly distributed on the Au surface. Further XPS analysis presented in Fig. 2E reveals that the Au maintains the metallic state, while the binding energy of Hg4f orbital presents two main peaks at 100.2 eV and 104.6 eV corresponding to $Hg4f_{7/2}$ and $Hg4f_{5/2}$, respectively which suggested only Hg^0 can be distinguished from the Au surface (Fig. 2F). Hence the Hg(I) can be further reduced to Hg(0) on the gold surface.

The aforementioned results demonstrated that the Hg^{2+} can be directly reduced to Hg^0 by Au thin film and do not require the cooperation of reductive ligands. This reaction was in consistent with the anti-Galvanic reaction (AGR) and follows the path of Hg(II) → Hg(I) → Hg(0) which was firstly described for AGR reaction. However, such reaction occurs in Au films was not in line with the typical pattern that AGR could only happens between Hg^{2+} and smaller Au NPs with size less than 3 nm.[16] Hence it could be concluded that AGR can also take place between Hg^{2+} and Au films in bulk state.

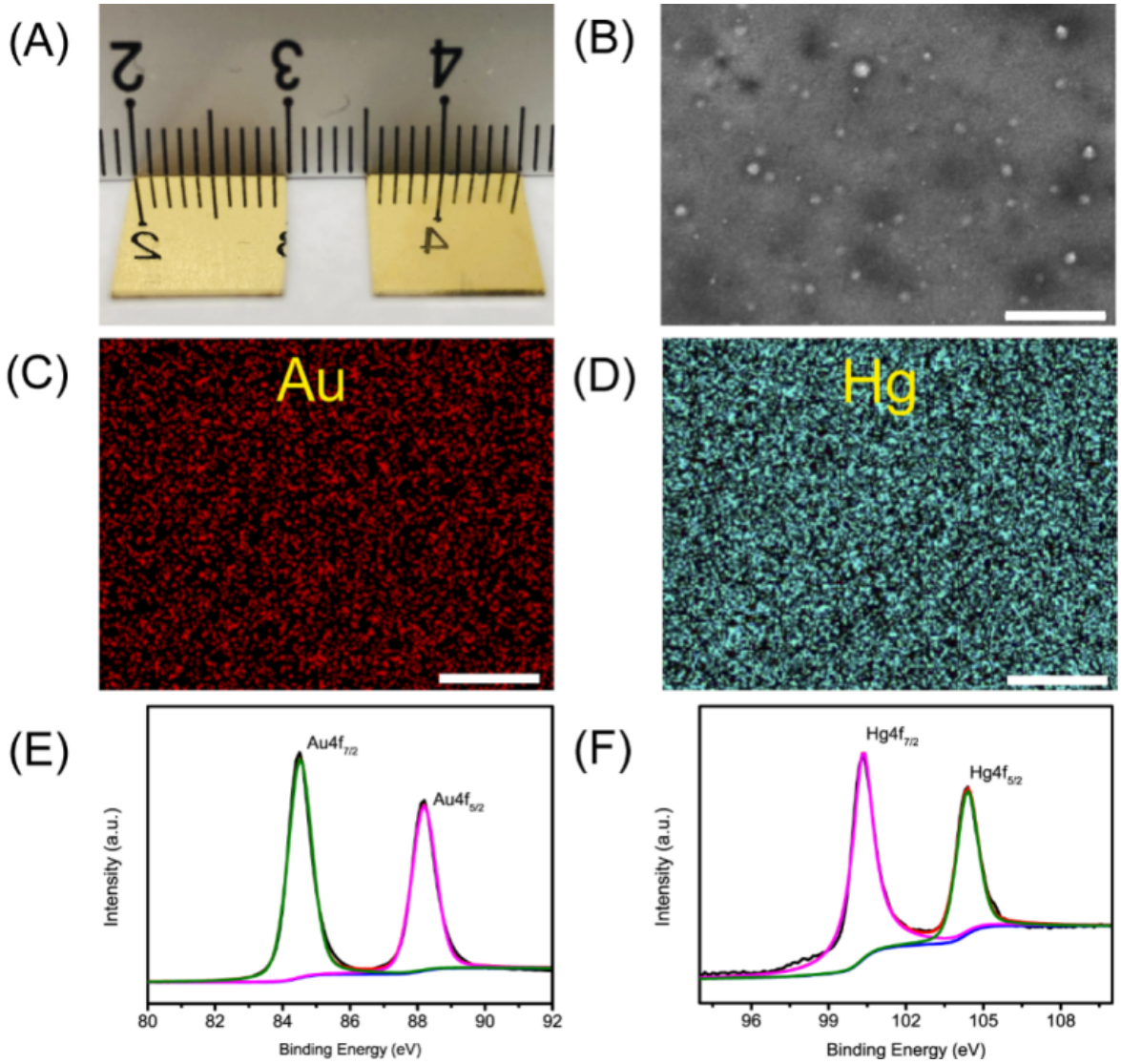

Figure 2. (A) Photograph of a thin gold layer before (left) and after (right) $Hg(NO_3)_2$ treatment. (B) SEM image of the gold surface after treatment with $Hg(NO_3)_2$ (scale bar: 1 μm) and its corresponding EDX mapping of Au (C) and Hg (D). The Hg/Au ratio as determined by EDX is 12.3%. Deconvoluted XPS core level spectra of Au4f (E) and Hg4f (F) of the $Hg(NO_3)_2$ treated gold sample. The Hg/Au ratio calculated from XPS result of the sample is 10.16%.

Since the surfaces of gold thin films with $HgCl_2$ and $Hg(NO_3)_2$ treatment are dominated by different mercury species, they may have different impacts on the enzyme-mimicking activity of gold. Therefore, the effects of the generated Hg^+ or Hg^0 on the enzyme-mimetic activities of the gold layer were investigated. Neither the $HgCl_2$-treated nor untreated gold layers exhibited any obvious peroxidase activity, but the $Hg(NO_3)_2$-treated gold layer did (Fig. 3A). In order to test their catalase-like reaction after treatment, an aqueous H_2O_2 solution (30 wt%) was dropped directly on the Au surfaces. Surprisingly, the treated gold surfaces (regardless of whether with $HgCl_2$ (Video1 in SI) or $Hg(NO_3)_2$) (Video2 in SI) vigorously decomposed H_2O_2 with violent bubbling of generated O_2 gas. In contrast, no visible gas bubbling was observed on the untreated sample. This indicates the remarkable enhancement in catalase-like activity of Au film with Hg^{2+} treatment. The catalase activity was further determined by a typical spectroscopic method. Consistent with the visible result, UV-vis spectroscopy shows that the bare Au film is almost inactive in catalyzing H_2O_2 decomposition, while a significant H_2O_2 decomposition behavior can be achieved for both $HgCl_2$ and $Hg(NO_3)_2$ treated samples (Fig. 3B). Hence it can be concluded that the Hg^+ might not, but Au@Hg amalgam did stimulate the peroxidase activity of the bare gold layer. It is possible that, as already observed by another group[17], the interactions between Hg^{2+} or Hg^+ with Au are inhibitory for the peroxidase-mimicking activity. Inspired by these observations, the control the stepwise reduction of Hg^{2+} on gold surface can be acted as a feasible avenue to selectively tune its peroxidase- and catalase-like activities. Moreover, it worth noting that nanomaterials in bulk state should be inert as enzyme mimetics, but the modified Au films in this work still exhibit excellent enzyme-mimicking activity, which is a surprising finding and may broaden their application range in real biomedical application.

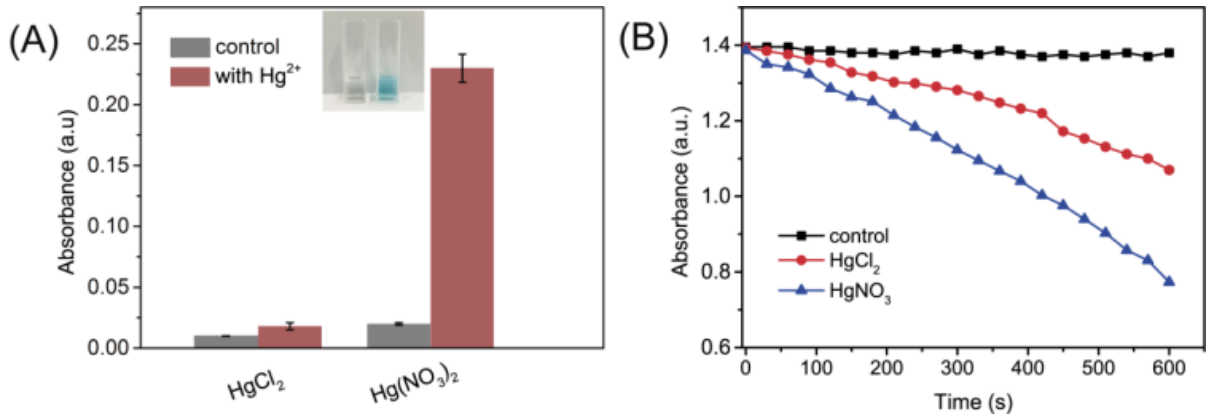

Figure 3. (A) Peroxidase-like and (B) catalase-like activities of treated and control samples.

Based on the above discussion, it is obvious the Hg^{2+}-treated gold thin layer could accelerate both the peroxidase and catalase activities of Au, due to the formation of Au@Hg on the Au surfaces. But the activation effect by Au@Hg remains unclear. Hence, we performed DFT calculations to examine the mechanisms responsible for the peroxidase and catalase activity enhancement. Our calculations suggest the following two-step reactions for the peroxidase-like activity of Au(111)@Hg.[18]

$H_2O_2^* = 2OH^*$ (1)

$2OH^* = H_2O^* + O^*$ (2)

The O* adatom formed via the above reactions easily oxidizes the TMB substrate, providing Au(111)@Hg with peroxidase-like activity. As shown in Fig. 4A, H_2O_2 prefers to adsorb in the vicinity of a Hg atom on the Au(111) surface, with an adsorption energy of −0.15 eV (see structure a_1). In sharp contrast, the adsorption of H_2O_2 on a pure Au(111) surface is thermodynamically unfavorable, with a positive adsorption energy of 0.11 eV.[18] The Hg atom greatly increases the affinity of the Au surface to H_2O_2. In addition, the rate-determining step on Au(111)@Hg is the cleavage of the H_2O_2's O-O bond (i.e., a_1−b_1−c_1),

which has a small energy barrier of only 0.26 eV. However, converting H_2O_2* to a O* adatom on the pure Au(111) surface has a higher energy barrier of 0.6 eV. The easier adsorption and activation of H_2O_2 on Au(111)@Hg than on pure Au(111) agree well with the observed enhanced peroxidase-like activity of the former.

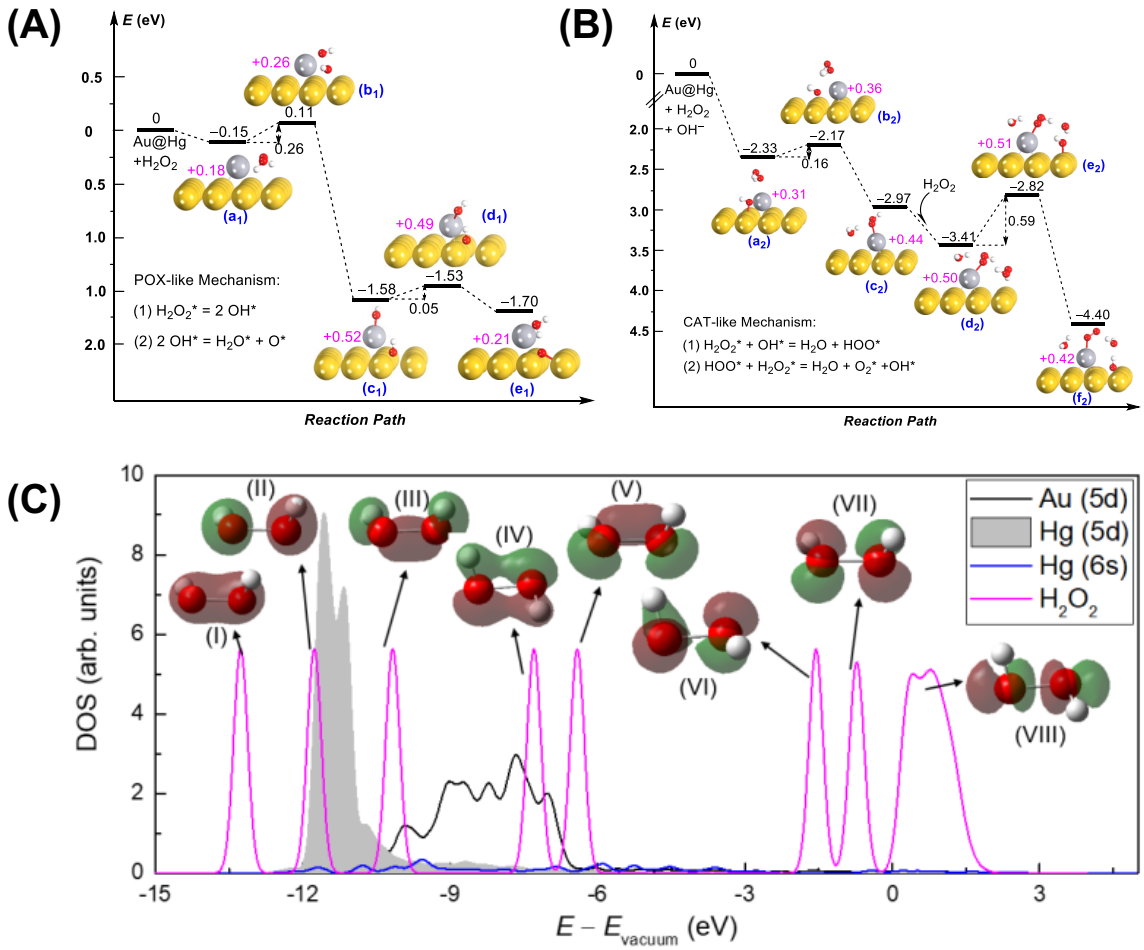

Figure 4. DFT-calculated potential energy profile along the reaction path of Au(111)@Hg exhibiting peroxidase-like activity (A) and catalase-like activity (B). The yellow atoms denote Au, grey atoms denote Hg, red atoms denote H and white atoms denote O. (C) Calculated projected density of states (PDOS) of Au(111)@Hg and total density of states of H_2O_2.

Similarly, the enhanced catalase-like activity of Au(111)@Hg can be ascribed to the stronger adsorption of H_2O_2 on the surface and the lower energy barrier for H_2O_2 to be

decomposed into O_2 and H_2O. The Au(111)@Hg with a pre-adsorbed OH^- is the active site for the catalase-like activity, catalyzing the decomposition of H_2O_2 via the following reactions.

$$H_2O_2^* + OH^* = HO_2^* + H_2O^* \quad (3)$$

$$H_2O_2^* + HO_2^* = O_2^* + OH^* + H_2O^* \quad (4)$$

As shown in Fig 4B, the energy for the co-adsorption of OH and H_2O_2 on Au(111)@Hg is −2.33 eV, which is more negative than the −2.07 eV calculated for pure Au(111).[18] The rate-determining step for Au(111)@Hg, i.e., the formation of the second H_2O molecule (d_2−e_2−f_2), has an energy barrier of 0.59 eV, which is lower than the 0.8 eV calculated for pure Au(111).[18]

To further study the role of the Hg atom in enhancing the peroxidase- and oxidase-like activities of Au@Hg, Fig. 4C plots the projected density of states (PDOS) for structure $\mathbf{a_1}$ in Fig. 4A. As shown in Fig. 4C, Hg (5*d*) orbitals are located in the energy window from −12 eV to −10 eV, and Au (5*d*) from −10 eV to −6 eV. The PDOS peaks corresponding to the O-O bonding orbital (I), O-O anti-bonding orbital (VIII), O-H bonding orbitals (II, III), and non-bonding electron lone pairs (IV, V, VI, VII) for H_2O_2 are also shown in Fig. 4C. Obviously, Hg (5*d*) is energetically closer to H_2O_2's bonding orbitals (I, II, III) than Au (5*d*). The match of energy levels of Hg (5*d*) and H_2O_2's bonding orbitals is the underlying reason for the ability of Hg to enhance the peroxidase and catalase-like activities of Au(111) surfaces. These DFT calculations support strongly the activation effect by Au@Hg amalgam.

4. Conclusions

In this study, the interaction between gold and Hg^{2+} originated from different source was systematically investigated by using a bare gold layer as the substrate. Basing on our results, it can be proposed that a direct AGR happens between Hg^{2+} and Au, which follows the

reduction path of Hg(II)->Hg(I)->Hg(0). The investigations on the nanozymatic activities of treated gold reveal that, for $Hg(NO_3)_2$ treated Au films, both greatly boosted peroxidase and catalase activities can be achieved due to formation of Au@Hg amalgam, while only catalase-like activity acceleration for $HgCl_2$ treated ones due to its major Hg^+ species on Au surface. These finds provides an effective strategy to specifically regulate the peroxidase or catalase activity of gold by controlling the stepwise reduction of Hg^{2+} introduced from different source. As demonstrated by the Further density functionality theory (DFT) calculations, it is the significantly lowered activation energy by Au@Hg amalgam that responsible for the acceleration of both peroxidase and catalase reaction. The exciting results obtained in this study will pave way for the design of nanozymes with specific activity, as well as the field expansion in practical applications.

Supporting Information

Supporting Information is available from the Wiley Online Library or from the author. XRD, SEM and EDX data are provided.

Acknowledgements

This work was financially supported by the National Natural Science Foundation of China (31971315), the Fundamental Research Funds for the Central Universities (3102017OQD048, 3102017OQD049), the China Postdoctoral Science Foundation (2018M633566) and the Postdoctoral Science Foundation of Shaanxi (2018BSHQYXMZZ35). M.K. is grateful for funding from the Spanish Ministry of Economy and Competitiveness (MINECO) [MAT2016-77393-R], including FEDER funds, and the Maria de Maeztu Units of Excellence Programme [MDM-2016-0618]. We would like to thank the Analytical & Testing Centre of Northwestern Polytechnical University for electron microscopy.

References

[1] L. Gao, J. Zhuang, L. Nie, J. Zhang, Y. Zhang, N. Gu, T. Wang, J. Feng, D. Yang, S. Perrett, X. Yan, *Nat Nanotechnol* **2007**, 2, 577.

[2] a) Y. Liu, H. Wu, Y. Chong, W. G. Wamer, Q. Xia, L. Cai, Z. Nie, P. P. Fu, J. J. Yin, *ACS Appl Mater Interfaces* **2015**, 7, 19709; b) J. Liu, L. Meng, Z. Fei, P. J. Dyson, L. Zhang, *Biosens Bioelectron* **2018**, 121, 159.

[3] a) Y. Hu, X. J. Gao, Y. Zhu, F. Muhammad, S. Tan, W. Cao, S. Lin, Z. Jin, X. Gao, H. Wei, *Chem. Mater* **2018**, 30, 6431; b) W. He, X. Wu, J. Liu, X. Hu, K. Zhang, S. Hou, W. Zhou, S. Xie, *Chem Mater* **2010**, 22, 2988.

[4] a) B. Jiang, L. Yan, J. Zhang, M. Zhou, G. Shi, X. Tian, K. Fan, C. Hao, X. Yan, *ACS Appl Mater Interfaces* **2019**, 11, 9747; b) N. Singh, M. A. Savanur, S. Srivastava, P. D'Silva, G. Mugesh, *Angew Chem Int Ed Engl* **2017**, 56, 14267.

[5] a) X. Mu, J. Wang, Y. Li, F. Xu, W. Long, L. Ouyang, H. Liu, Y. Jing, J. Wang, H. Dai, Q. Liu, Y. Sun, C. Liu, X. D. Zhang, *ACS nano* **2019**, 13, 1870; b) M. Moglianetti, E. De Luca, D. Pedone, R. Marotta, T. Catelani, B. Sartori, H. Amenitsch, S. F. Retta, P. P. Pompa, *Nanoscale* **2016**, 8, 3739; c) X. H. Zhimei He, Chen Wang, Xiangli Li, Yijing Liu,, S. W. Zijian Zhou, Fuwu Zhang, Zhantong Wang, Orit, J.-J. Z. Jacobson, Guocan Yu, Yunlu Dai, and Xiaoyuan, C. F. Chen, *Angew Chem Int Ed* **2019**, 58, 8752.

[6] a) H. Wei, E. Wang, *Chem Soc Rev* **2013**, 42, 6060; b) J. Wu, X. Wang, Q. Wang, Z. Lou, S. Li, Y. Zhu, L. Qin, H. Wei, *Chem Soc Rev* **2019**, 48, 965.

[7] a) R. Long, K. Mao, X. Ye, W. Yan, Y. Huang, J. Wang, Y. Fu, X. Wang, X. Wu, Y. Xie, Y. Xiong, *J Am Chem Soc* **2013**, 135, 3200; b) Z. Li, X. Yang, Y. Yang, Y. Tan, Y. He, M. Liu, X. Liu, Q. Yuan, *Chemistry* **2018**, 24, 409; c) M. Vazquez-Gonzalez, W.

C. Liao, R. Cazelles, S. Wang, X. Yu, V. Gutkin, I. Willner, *ACS nano* **2017**, 11, 3247; d) Z. Zhang, X. Zhang, B. Liu, J. Liu, *J Am Chem Soc* **2017**, 139, 5412.

[8] a) W. He, Y. Liu, J. Yuan, J. J. Yin, X. Wu, X. Hu, K. Zhang, J. Liu, C. Chen, Y. Ji, Y. Guo, *Biomaterials* **2011**, 32, 1139; b) S. Singh, P. Tripathi, N. Kumar, S. Nara, *Biosensors & bioelectronics* **2017**, 92, 280; c) C. Schopf, A. Martín, M. Schmidt, D. Iacopino, *J Mater Chem C* **2015**, 3, 8865; d) X. n. L. p. Isaac Ojea-Jime´nez, Jordi Arbiol, Victor Puntes, *ACS Nano* **2012**, 6, 2253.

[9] a) X. Jiang, W. Xu, X. Chen, Y. Liang, *Anal Methods* **2019**, 11, 2179; b) Cheng-Yan Lin, Cheng-Ju Yu, Yen-Hsiu Lin, W.-L. Tseng, *Anal Chem* **2010**, 82, 6830; c) L. Tan, Y. Zhang, H. Qiang, Y. Li, J. Sun, L. Hu, Z. Chen, *Sens Actuators B* **2016**, 229, 686.

[10] C. W. Lien, Y. C. Chen, H. T. Chang, C. C. Huang, *Nanoscale* **2013**, 5, 8227.

[11] a) G. Kresse, J. Furthmuler, *Phys Rev B* **1996**, 54, 1169; b) G. Kresse, D. Joubert, *Phy Rev B* **1999**, 59, 1758; c) G. Kresse, J. Furthmiiller, *Computational Mater Sci* **1996**, 15.

[12] J. P. Perdew, K. Burke, M. Ernzerhof, *Phys Rev Lett* **1996**, 77, 3865.

[13] P. E. Blochl, *Phys Rev B Condens Matter* **1994**, 50, 17953.

[14] M. Methfessel, A. T. Paxton, *Phys Rev B Condens Matter* **1989**, 40, 3616.

[15] H. J. Monkhorst, J. D. Pack, *Phys Rev B* **1976**, 13, 5188.

[16] a) Z. Gan, N. Xia, Z. Wu, *Acc Chem Res* **2018**, 51, 2774; b) X. Liu, D. Astruc, *Adv. Mater.* **2017**, 29; c) L. Liao, S. Zhou, Y. Dai, L. Liu, C. Yao, C. Fu, J. Yang, Z. Wu, *J Am Chem Soc* **2015**, 137, 9511.

[17] Z. Rui, Z. Yan, X. Wang, L. Liang, Y. Long, Q. Wang, H. Zhang, X. Huang, H. Zheng, *Talanta,* **2013**, 117, 127.

[18] J. Li, W. Liu, X. Wu, X. Gao, *Biomaterials* **2015**, 48, 37.

1

The peroxidase and catalase activity of gold can be precisely regulated by controlling the stepwise reduction of Hg^{2+} from different source on gold surface.

Keyword: Au nanozyme, mercury treatment, Au@Hg amalgam, nanozymatic activity, activity specificity adjustment

Control of Stepwise Hg^{2+} Reduction on Gold to Selectively Tune Its Peroxidase and Catalase-like Activities and the Mechanism

Yao Chen,[a,‡] Xiaomei Shen,[b,‡] Unai Carmona,[c] Fan Yang,[c] Xingfa Gao,*[,b] Mato Knez*[,c] and Lianbing Zhang*[,a], Yong Qin[a]

Corresponding authors: gaox@jxnu.edu.cn, m.knez@nanogune.eu, lbzhang@nwpu.edu.cn

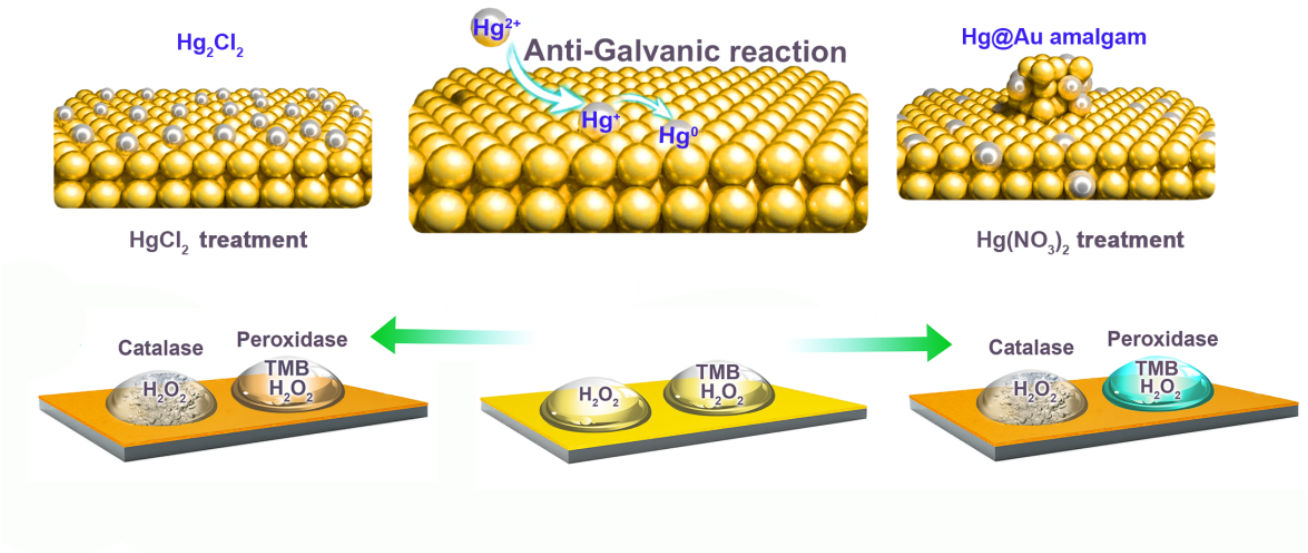

Supporting Information

Yao Chen,[a,‡] Xiaomei Shen,[b,‡] Unai Carmona,[c] Fan Yang,[c] Xingfa Gao,*[,b] Mato Knez*[,c] and Lianbing Zhang*[,a], Yong Qin[a]

Corresponding authors: gaox@jxnu.edu.cn, m.knez@nanogune.eu, lbzhang@nwpu.edu.cn

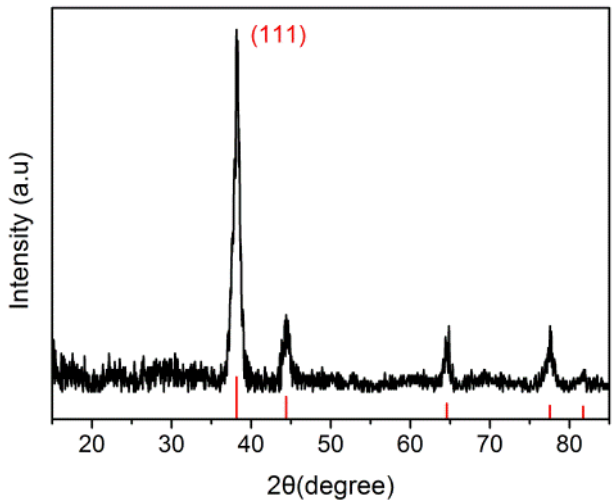

Fig S1. XRD spectrum of the bare thin gold film.

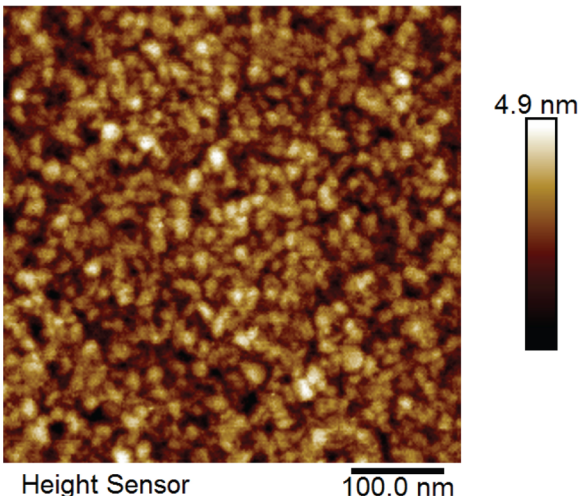

Fig S2. AFM image of bare gold layer.

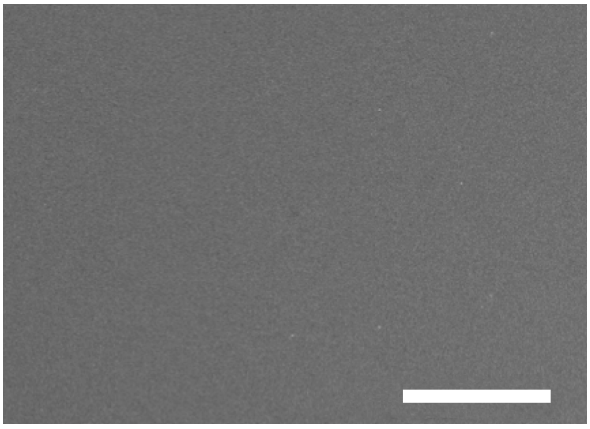

Fig S3. SEM image of a sputtered thin gold layer, scale bar: 50 μm.

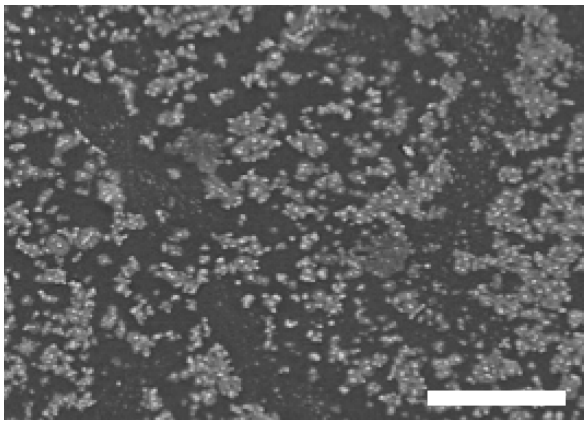

Fig S4. SEM image of a treated gold layer after incubation in water for a week, scale bar: 5 μm.

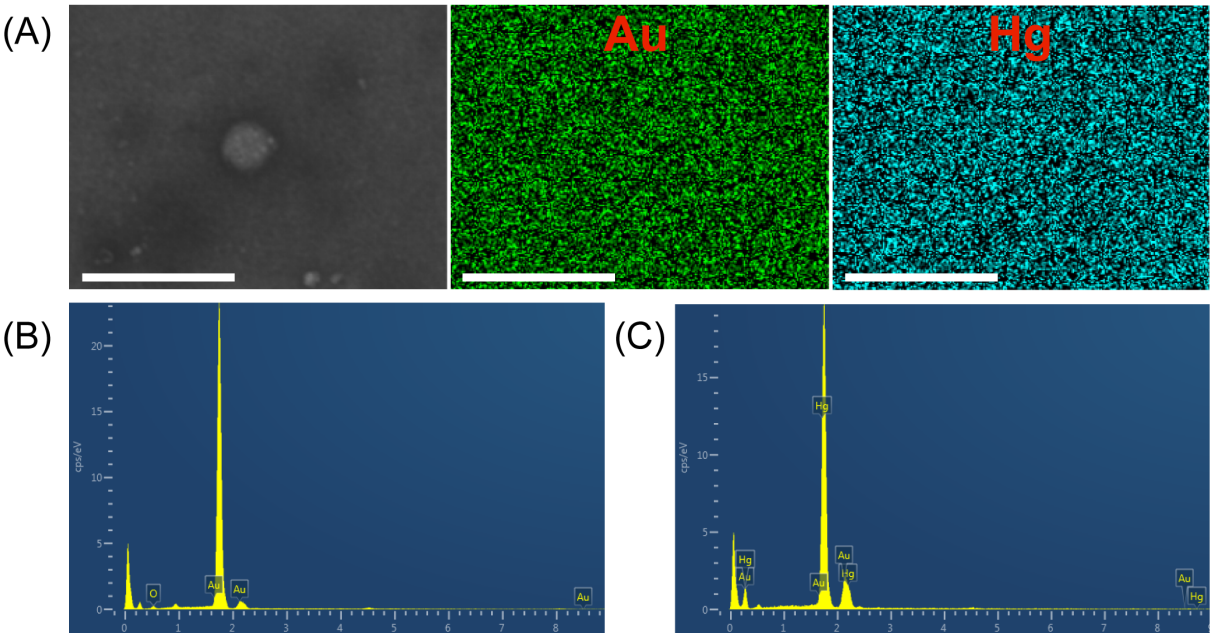

Fig S5. (A) SEM image of the $HgCl_2$ treated sample and its corresponding EDX mapping of Au and Hg. Scale bar: 5 μm. EDX spectra of a thin gold layer before (B) and after (C) treatment with $HgCl_2$. The Hg/Au ratio is 9.05%.